

*“Experiments are the poets of science,
they unravel the mysteries with a symphony of data and insight.”*

– Marie Curie

4

Probing Detector Sensitivity Through Synergy of DUNE, T2HK and T2HKK

Combining data from different neutrino experiments is of paramount importance in advancing our understanding of neutrino properties and behaviors. Neutrinos are notoriously challenging to study due to their weak interactions and elusive nature, which necessitates the use of a variety of experimental techniques and setups. By pooling data from diverse experiments, researchers can enhance the statistical significance of their findings, leading to more precise measurements and reduced uncertainties. Moreover, different experiments often have distinct systematic uncertainties and limitations, and combining their data can help mitigate these issues and provide a more comprehensive view of neutrino phenomena. This collaborative approach also facilitates cross-verification of results, reducing the likelihood of experimental biases and errors. Ultimately, combining data from various experiments allows scientists to draw more robust conclusions about neutrino oscillations, masses, mixing angles, and potential beyond-the-Standard-Model effects, pushing the boundaries of our knowledge in the fascinating realm of neutrino physics.

4.1 Importance of combing data from various experiments

The revelation of neutrino oscillations, jointly pioneered by Super-Kamiokande (SK)[1] and Sudbury Neutrino Observatory (SNO)[2], has ushered in a new era of probing physics beyond the Standard Model (BSM). Neutrino oscillations have unequivocally demonstrated that neutrinos possess mass, marking a significant experimental hint of BSM physics. Various neutrino experiments [3–6] have been diligently investigating the parameters related to neutrino oscillations. Neutrinos offer a promising avenue to explore BSM phenomena in the leptonic sector. BSM models that elucidate neutrino masses and mixing often introduce non-standard interactions (NSIs), representing novel couplings of neutrinos. Given the exceptional accuracy and precision of ongoing and forthcoming neutrino experiments, these subtle effects in neutrino oscillations can wield a substantial influence on the scientific potential of these endeavors. This study delves into the ramifications of scalar-mediated NSIs on the determination of the leptonic phase δ_{CP} within three long baseline (LBL) neutrino experiments: DUNE [81], T2HK [82], and T2HKK [83]. By synergistically analyzing these LBL experiments, we unveil the model-independent impact of scalar NSIs.

The ongoing and upcoming neutrino experiments strive to achieve the utmost precision in measuring neutrino oscillation parameters. However, the presence of parameter degeneracies among the mixing parameters introduces challenges to the accurate determination of these parameters [150–153]. These degeneracies lead to scenarios where multiple sets of mixing parameters yield identical oscillation probabilities, causing ambiguity in identifying the true values of the parameters. To mitigate these effects, combining data from diverse experiments becomes necessary. The degenerate parameter space varies across different neutrino experiments, and the synergy between such experiments can aid in the unambiguous determination of oscillation parameters [151–154]. The combination of multiple experiments not only enhances sensitivity but also reveals potential synergies among them. This approach is vital for resolving the degeneracies and accurately determining neutrino oscillation parameters [155]. For instance, in the presence of a light sterile neutrino, a combination of three different long baseline (LBL) experiments (DUNE, T2HK, T2HKK) exhibits superior sensitivity (beyond 5σ) for CP-violation measurements compared to individual experiments [155]. Similarly, the combination of experiments has been shown to improve mass hierarchy and octant discovery potential sensitivities [155]. Moreover, combining experiments can address

challenges such as mass hierarchy- δ_{CP} degeneracy [156] and vector non-standard interactions [157], enhancing the precision of CP-violation and other measurements in the leptonic sector. The synergy between experiments, like T2HK and JUNO [158], can yield significant improvements in neutrino mass ordering determination. The combination of T2K and NO ν A has been demonstrated to resolve θ_{23} octant ambiguities, regardless of the hierarchy and δ_{CP} [85]. The synergy between diverse neutrino experiments is harnessed to deepen our understanding, optimize knowledge of neutrino oscillations, and enhance the overall physics potential [159–168].

In the era of precision neutrino physics, ongoing and upcoming experiments prioritize accurate measurements of neutrino mixing parameters. These experiments seek to address three main unknowns in the neutrino sector: neutrino mass hierarchy [84], mixing angle θ_{23} octant [85], and the CP phase (δ_{CP}) determination in the leptonic sector [86]. These experiments possess robust capabilities to detect subdominant neutrino effects, such as Non-Standard Interactions (NSIs), which can significantly impact oscillation parameter measurements. Initially proposed with vector mediators coupling neutrinos to environmental fermions, NSIs have been explored widely [55–58, 87] and stand as candidates to probe physics beyond the Standard Model. The effects of vector-mediated NSIs can notably influence the physics potential of diverse neutrino experiments [88–112], with ongoing investigations [113–129]. A comprehensive overview of vector NSI parameter bounds is available in [130, 131].

This exploration delves into the non-standard coupling of neutrinos with a scalar [7, 8, 145, 146]. The scalar-mediated NSI introduces unique phenomenology in neutrino oscillations by influencing the neutrino mass term in the Hamiltonian. Unlike vector NSIs, the effects of scalar NSIs scale linearly with environmental matter density, making long-baseline neutrino experiments particularly suitable for probing them. Initial concepts of scalar NSIs aimed to fit recent data from the Borexino experiment [7]. While stringent bounds on scalar NSI parameters are currently lacking, some studies have explored constraints under astrophysical and cosmological limits [11, 147]. Our work [8] explores the potential impact of scalar NSIs on CP-violation sensitivities in long baseline experiments, with DUNE as a case study. The presence of scalar NSIs notably affects DUNE’s CP sensitivities, motivating further exploration of scalar NSIs in long baseline experiments. Combining various long baseline experiments becomes pivotal, as synergy studies enhance the precision of sensitivity scenarios.

In this study, we conduct a novel synergy analysis to examine the impacts of scalar NSIs on three long baseline experiments: DUNE, T2HK, and T2HKK. Our approach is

model-independent, focusing on the effects of scalar NSIs individually. Notable consequences of scalar NSIs emerge in the sensitivities of these neutrino experiments, particularly in relation to CP-violation (CPV) effects. Through combined analyses of DUNE with T2HK and DUNE with T2HKK, we explore potential synergies among these experiments. Our findings reveal that specific negative NSI parameter values consistently suppress CPV sensitivities. Conversely, positive NSI parameters can mimic standard CPV effects, closely resembling DUNE and T2HKK's inherent CPV sensitivities. The joint consideration of LBL experiments (DUNE+T2HK and DUNE+T2HKK) enhances overall sensitivities and helps mitigate the underlying CPV measurement ambiguities. As a consequence, constraining these NSI parameters remains imperative for ensuring precise measurements and robust interpretation of data from diverse neutrino experiments.

To examine the influence of NSIs across various neutrino experiments, we employed the Global Long Baseline Experiment Simulator (GLoBES) [138, 148, 149]. Our simulation studies adopted mixing parameter values outlined in table 3.1. Throughout our analysis, we adopted the normal hierarchy as the true hierarchy and the higher octant as the true octant. The scope of our investigation encompassed three proposed super-beam experiments: DUNE, T2HK, and T2HKK, with systematic and background information derived from the respective Technical Design Reports (TDRs). The uncertainties associated with signals and backgrounds are summarized in table 2.2. Notably, we scrutinized individual diagonal scalar NSI elements in this study. Initially, we assessed the impact of scalar NSIs at both probability and event levels within the detector. Subsequently, we analyzed the influence of scalar NSIs on the CP asymmetry parameter. The ensuing subsections detail the technical specifics of the three experiments, including the repercussions of scalar NSIs on oscillation probabilities and the CP asymmetry parameter.

4.2 Effects on oscillation probabilities

In this segment, we delve into the ramifications of scalar NSIs on neutrino oscillation probabilities, focusing on the three diagonal cases outlined in equations 2.16, 2.17, and 2.18. To undertake this analysis, we harnessed the NuOscProbExact package [16]. By adopting the neutrino Hamiltonian according to equation 2.11, and encompassing the three scalar NSI cases, we executed the analysis. Our oscillation parameter inputs aligned with those documented in table 3.1. In our assessments, we typically assumed

the normal hierarchy (NH) as the true mass hierarchy and the higher octant (HO) as the accurate octant unless specifically noted otherwise.

In figure 4.1, we present the impact of diagonal scalar NSI elements η_{ee} (left column), $\eta_{\mu\mu}$ (middle column), and $\eta_{\tau\tau}$ (right column) on $P_{\mu e}$ across the neutrino energy spectrum. The depiction encompasses various baselines: DUNE (top row), T2HK (middle row), and T2HKK (bottom row). These probabilities were computed for $\delta_{CP} = -90^\circ$ and $\theta_{23} = 47^\circ$. In the visualizations, the solid red line corresponds to the absence of scalar NSI ($\eta_{\alpha\beta} = 0$). Additionally, the black, blue, and magenta solid (dashed) lines depict the impact of chosen positive (negative) values of η_{ee} , $\eta_{\mu\mu}$, and $\eta_{\tau\tau}$, respectively. It's notable that,

- The existence of scalar NSI parameters introduces notable alterations in the oscillation probabilities across all three baselines, particularly near the points of oscillation maxima.
- In the case of η_{ee} , positive (negative) values lead to heightened (diminished) probabilities around the oscillation maxima. Conversely, for $\eta_{\tau\tau}$, positive (negative) values evoke contrasting changes.
- For $\eta_{\mu\mu}$, positive (negative) values induce a shift of the oscillation maxima towards higher (lower) energy ranges, accompanied by slight amplitude suppression.

The intriguing manifestations of scalar NSI in neutrino oscillations prompt us to delve deeper, extending our investigation to the construction of a CP-asymmetry parameter at the probability level.

4.3 Effects on CP-asymmetry

In this study, our primary focus is on investigating the potential influence of scalar NSI on the capability to measure CP-violation in the three selected long-baseline experiments. We construct the CP-asymmetry parameter at the level of probabilities as follows,

$$A_{CP} = \frac{P_{\mu e} - \bar{P}_{\mu e}}{P_{\mu e} + \bar{P}_{\mu e}}, \quad (4.1)$$

here, $P_{\mu e}$ and $\bar{P}_{\mu e}$ denote the appearance probabilities of ν_e and $\bar{\nu}_e$ respectively. The CP asymmetry parameter (A_{CP}) serves as an indicator of CP violation, quantifying the alteration in oscillation probabilities upon reversing the sign of the CP phase. The form

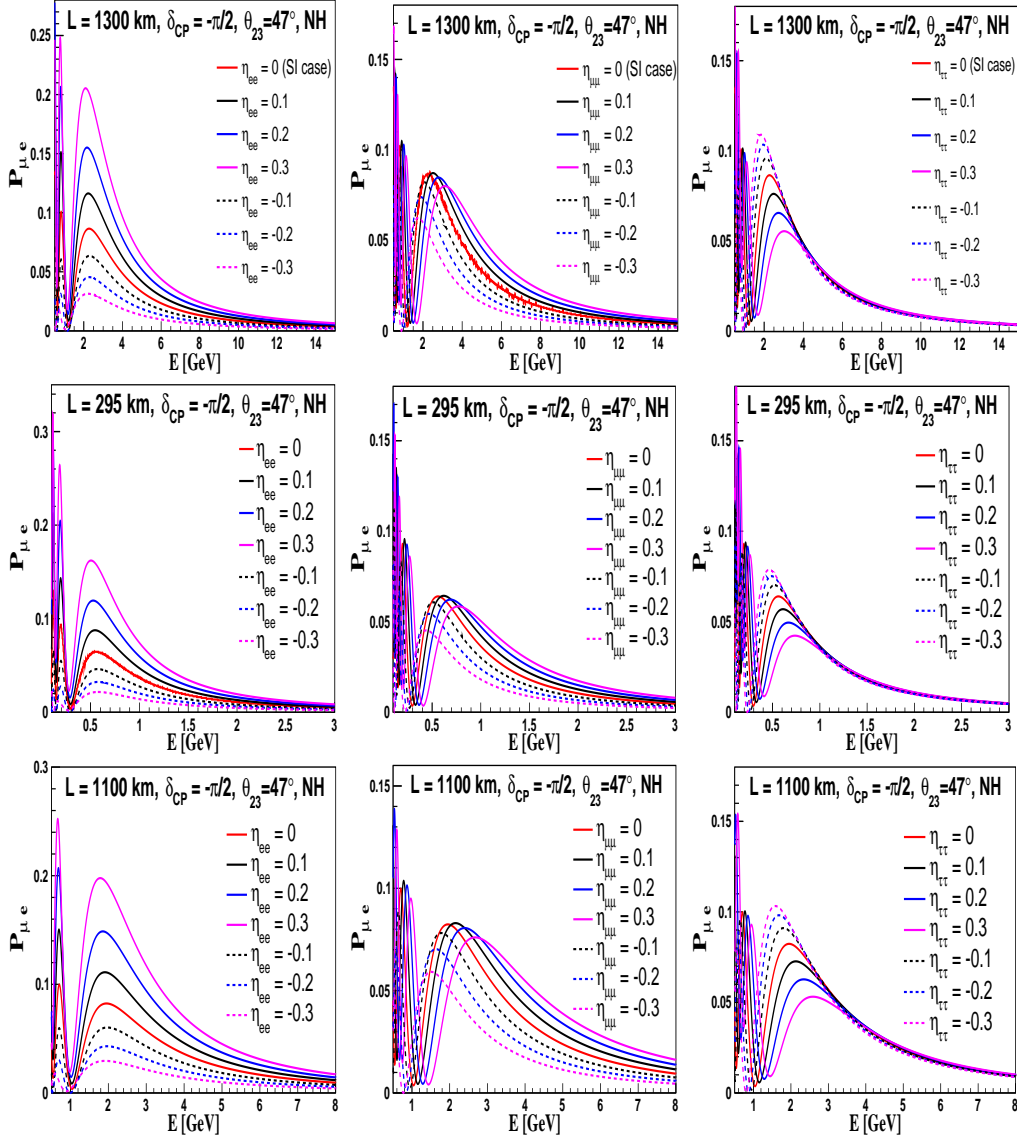


FIGURE 4.1: The effects of η_{ee} (left-column), $\eta_{\mu\mu}$ (middle-column) and $\eta_{\tau\tau}$ (right-column) on $P_{\mu e}$ at the baselines corresponding to DUNE (top-row), T2HK (middle-row) and T2HKK (bottom-row). Here, $\delta_{CP} = -\pi/2$, $\theta_{23} = 47^\circ$ and true mass Hierarchy = NH. In all the plots, the red solid-curve is for no-NSI case while other solid (dashed) curves are for positive (negative) NSI parameters.

and magnitude of the CP asymmetry curve are greatly influenced by the baseline and energy parameters.

Figure 4.2 displays the CP asymmetry in the presence of scalar NSI as a function of δ_{CP} for the respective baselines and peak energies of DUNE (left panel), T2HK (middle panel), and T2HKK (right panel). The peak energies for DUNE, T2HK, and T2HKK are set as 2.5 GeV, 0.5 GeV, and 0.66 GeV respectively. In all plots, the solid-red curve signifies the absence of scalar NSI, i.e., $\eta_{\alpha\beta} = 0$. The solid (dashed) curves in black, magenta, and green correspond to positive (negative) values of scalar NSI elements.

The following observations can be made from figure 4.2,

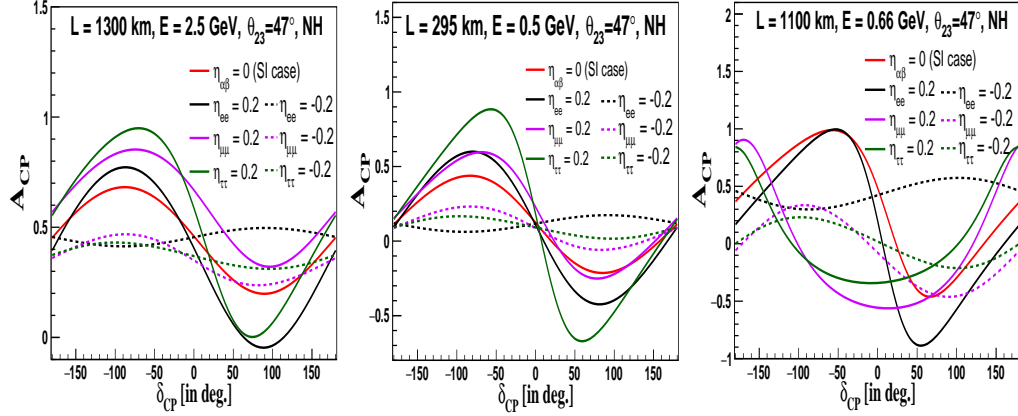


FIGURE 4.2: The CP–asymmetry vs δ_{CP} plot for DUNE (left–panel), T2HK (middle–panel) and T2HKK (right–panel) in presence of $\eta_{\alpha\beta}$ at corresponding peak energies. Here, $\theta_{23} = 47^\circ$ and true mass hierarchy = NH. In all the three plots, the solid–red curve is for no scalar NSI case and other coloured solid (dashed) curves are for chosen positive (negative) $\eta_{\alpha\beta}$.

- The presence of scalar NSI introduces degeneracies for various sets of $(\eta_{\alpha\beta}, \delta_{CP})$, which in turn impacts the anticipated CP asymmetry (A_{CP}) at DUNE, T2HK, and T2HKK.
- For DUNE, a positive η_{ee} amplifies A_{CP} within the δ_{CP} range of $[-150^\circ, 10^\circ]$, while a negative η_{ee} enhances it within $[0, 180^\circ]$. At T2HK, a positive (negative) η_{ee} augments (reduces) A_{CP} across the δ_{CP} range of $[-180^\circ, 0]$, whereas at T2HKK, positive η_{ee} mostly suppresses A_{CP} throughout the entire δ_{CP} range.
- In the case of DUNE, a positive $\eta_{\mu\mu}$ heightens A_{CP} across the entire δ_{CP} range. Negative $\eta_{\mu\mu}$ leads to enhanced A_{CP} between $\delta_{CP} = 60^\circ$ and 140° , with suppression elsewhere. At T2HK, positive (negative) $\eta_{\mu\mu}$ enhances (suppresses) A_{CP} between $\delta_{CP} = -180^\circ$ and 40° . T2HKK generally displays A_{CP} suppression with negative $\eta_{\mu\mu}$, while a fluctuating pattern is observed with positive $\eta_{\mu\mu}$.
- Regarding DUNE, a positive $\eta_{\tau\tau}$ enhances A_{CP} for $\delta_{CP} < 0$, crossing over and then suppressing within the δ_{CP} range of $[30^\circ, 140^\circ]$. A similar trend is observed at T2HK. For negative $\eta_{\tau\tau}$, A_{CP} remains moderately dependent on δ_{CP} at both DUNE and T2HK. T2HKK shows a substantial fluctuation in A_{CP} for both positive and negative $\eta_{\tau\tau}$.

4.4 Effects on the event rates

Driven by the notable influence on oscillation probabilities and A_{CP} , we shift our attention to investigating how scalar NSI affects event rates at the three detectors. Subsequently, we undertake a statistical exploration by formulating distinct χ^2 metrics to assess the impact of scalar NSI on δ_{CP} .

We proceed to offer a comprehensive examination of how scalar NSI parameters affect the binned event rates across the three LBL experiments. The visual representation in figure 4.3 underscores this discussion, showcasing the raw binned event rates for DUNE (left-panel), T2HK (middle-panel), and T2HKK (right-panel) with respect to the true neutrino energy. Our approach involves varying the $\eta_{\alpha\beta}$ parameters individually within the range of $[-0.3, 0.3]$, while maintaining δ_{CP} (true) at $-\pi/2$ and θ_{23} (true) at 47° .

To precisely explore the impact of scalar NSI on event rates, we introduce the parameter ΔN_{evt} , which is defined as:

$$\Delta N_{evt} = N_{evt}^{NSI} - N_{evt}^{SI}, \quad (4.2)$$

Where N_{evt}^{NSI} (N_{evt}^{SI}) signifies the binned event rates at the far detector of the experiment in the presence (absence) of scalar NSI. The values encapsulated by ΔN_{evt} provide a quantifiable measure of how scalar NSI influences the event rates. This analysis is further enriched in figure 4.4, where we present ΔN_{evt} as a function of neutrino energy and $\eta_{\alpha\beta}$ for DUNE (top-row), T2HK (middle-row), and T2HKK (bottom-row).

The interplay of figure 4.3 and figure 4.4 effectively reveals that,

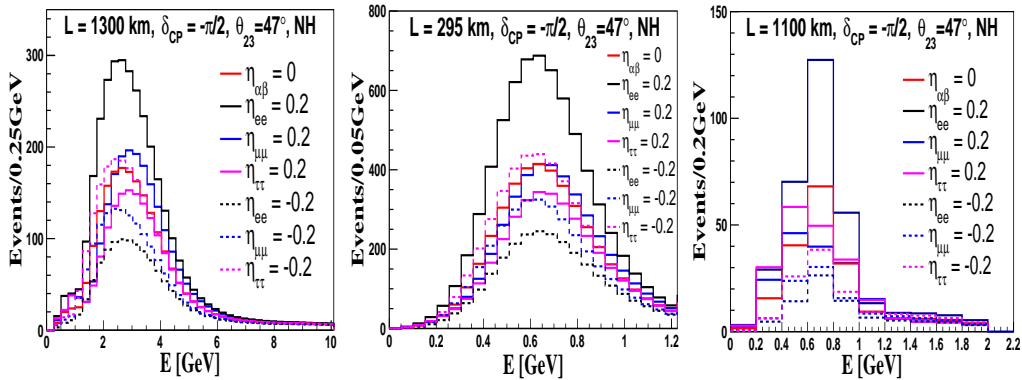


FIGURE 4.3: The binned event rates of DUNE (left), T2HK (middle) and T2HKK (right) as a function of neutrino energy at $\delta_{CP} = -\pi/2$, $\theta_{23} = 47^\circ$ and NH for different choices of $\eta_{\alpha\beta}$.

- A positive (negative) η_{ee} leads to an augmentation (reduction) in the binned event counts around the first oscillation maxima for DUNE and T2HK, and around the second oscillation maxima for T2HKK.

- On the other hand, the impact of $\eta_{\mu\mu}$ reveals a more intricate pattern in relation to energy. Positive and negative $\eta_{\mu\mu}$ values elicit fluctuating event rate changes across different energy ranges. For instance, considering positive $\eta_{\mu\mu}$, we observe heightened event rates within the energy range of [2.5 GeV, 5 GeV] at DUNE, whereas rates decrease within [1.5 GeV, 2.5 GeV]. For T2HK, enhanced (suppressed) rates appear within [2.0 GeV, 2.2 GeV] ([1 GeV, 1.8 GeV]), while T2HKK displays elevated (reduced) rates within [0.6 GeV, 1.2 GeV] ([0.3 GeV, 0.5 GeV]). Conversely, negative $\eta_{\mu\mu}$ yields an inverse energy variation trend across all three experiments.
- For $\eta_{\tau\tau}$, positive (negative) values predominantly diminish (enhance) event rates, particularly around the oscillation maxima, evident primarily in DUNE and T2HK. Nevertheless, a modest upturn in event rates occurs at certain lower energy ranges ([1 GeV, 2 GeV] for DUNE, [0.1 GeV, 0.3 GeV] for T2HK, and [0.2 GeV, 0.8 GeV] for T2HKK) when considering positive $\eta_{\tau\tau}$.
- The distinctive behaviors of the binned event rates portrayed in figure 4.3 align harmoniously with the patterns exhibited by neutrino oscillation probabilities, as demonstrated in figure 4.1.

Our attention now shifts towards investigating the potential influence of $\eta_{\alpha\beta}$ on the capacity of the three experiments to measure δ_{CP} . We conducted an analysis to assess the sensitivity of the experiments in constraining $\eta_{\alpha\beta}$. Additionally, we investigated how $\eta_{\alpha\beta}$ affects the measurements of CP-violation within these experiments. The CP-violation sensitivity is defined as the capacity of the experiments to discern between CP-conserving and CP-violating scenarios. Our approach involved marginalizing over systematic uncertainties. Initially, we determined the sensitivities for each individual experiment. Subsequently, we examined the synergistic effects by considering combinations such as DUNE+T2HK and DUNE+T2HKK. The outcomes of our study are discussed in the ensuing sections.

4.5 Sensitivity to scalar NSI parameters

In figure 4.5, we depict the experiments' capacity to constrain the scalar NSI parameters, $\eta_{\alpha\beta}$, for DUNE, T2HK, and the combined analysis of DUNE+T2HK. It's evident that both DUNE and T2HK can significantly constrain the NSI parameters, with the potential for further improvement in the joint analysis. The plots for η_{ee} , $\eta_{\mu\mu}$, and $\eta_{\tau\tau}$ are presented in the left, middle, and right panels, respectively. For the top (bottom)

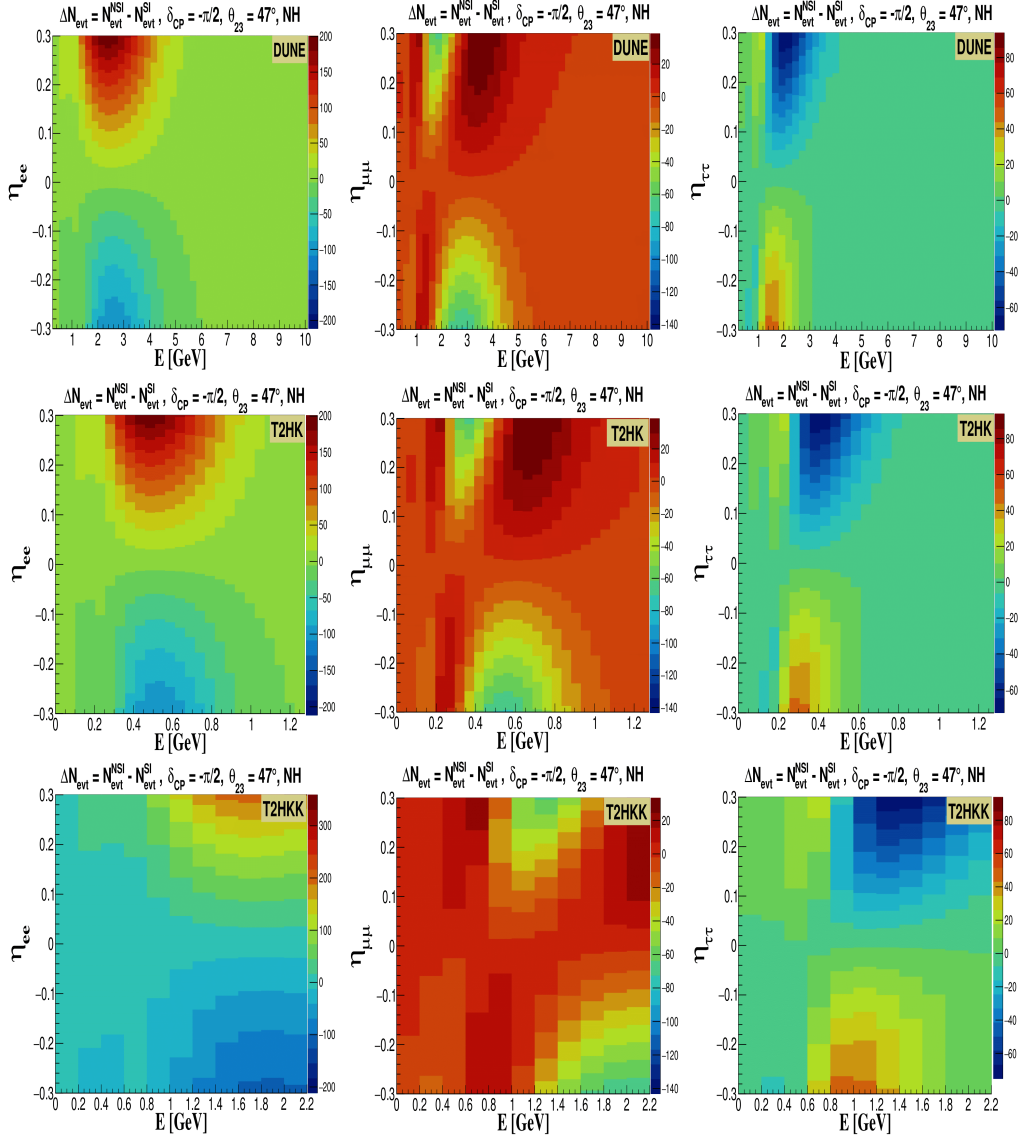


FIGURE 4.4: The variation of ΔN_{evt} of DUNE (top-row), T2HK (middle-row) and T2HKK (bottom-row) as a function of neutrino energy at fixed $\delta_{CP} = -\pi/2$, $\theta_{23} = 47^\circ$ and NH for different choices of $\eta_{\alpha\beta} \in [-0.3, 0.3]$. In the figure the left-column is for non-zero η_{ee} , the middle-column is for non-zero $\eta_{\mu\mu}$ and the right-column is for non-zero $\eta_{\tau\tau}$.

panel, we held the true values of $\eta_{\alpha\beta}$ fixed at 0.1 (-0.1) and marginalized the corresponding test $\eta_{\alpha\beta}$ values within the range of $[-0.5, 0.5]$. Throughout the analysis, we maintained the true neutrino mass hierarchy as normal and the true octant of θ_{23} as higher octant. Our analysis was based on a fixed true value of $\delta_{CP} = -90^\circ$ and true $\theta_{23} = 47^\circ$, unless otherwise specified. The resulting $\Delta\chi^2$ values were plotted against the test $\eta_{\alpha\beta}$ parameters. The dashed green and magenta lines signify the 3σ and 5σ confidence levels, respectively. Our observations indicate that,

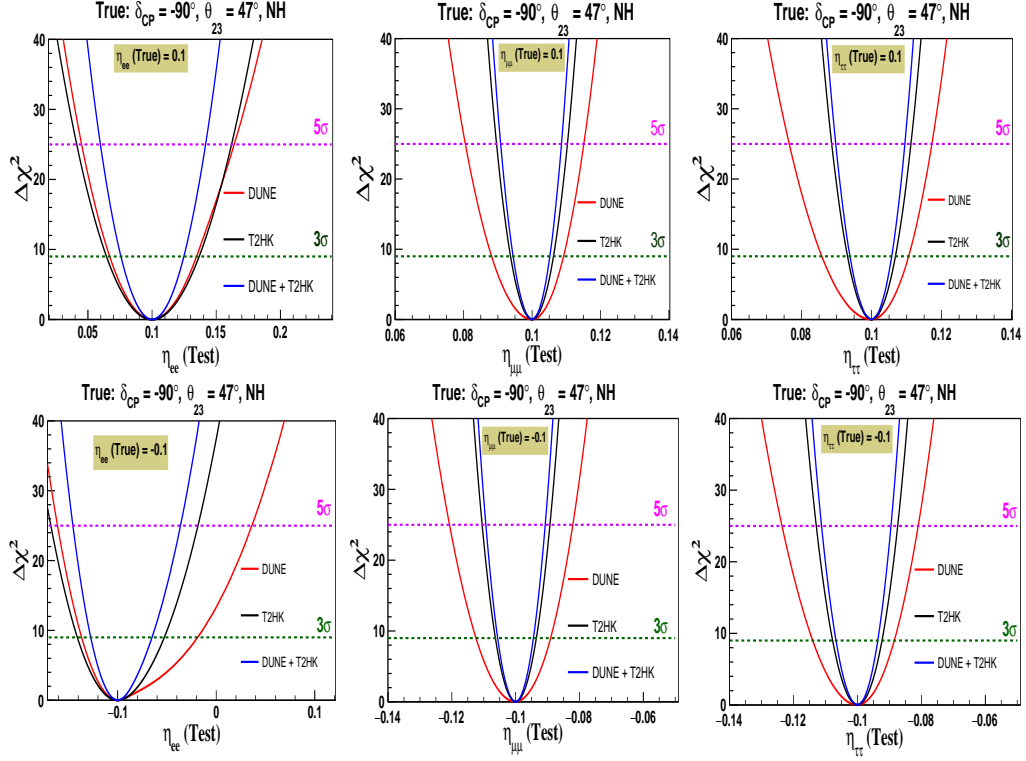


FIGURE 4.5: The sensitivity of DUNE, T2HK and DUNE + T2HK towards constraining non-zero η_{ee} (left-panel), $\eta_{\mu\mu}$ (middle-panel), and $\eta_{\tau\tau}$ (right-panel) at true $\delta_{CP} = -\pi/2$ and true $\theta_{23} = 47^\circ$. The top (bottom) panel is for true $\eta_{\alpha\beta} = 0.1$ (-0.1). In all the plots, the sensitivities for DUNE, T2HK and DUNE+T2HK are shown in red, black and blue respectively.

- When it comes to constraining η_{ee} (with a true value of $\eta_{ee} = 0.1$), DUNE exhibits slightly better sensitivity at the 3σ confidence level compared to T2HK. Conversely, T2HK demonstrates a more effective capacity to constrain $\eta_{\mu\mu}$ and $\eta_{\tau\tau}$ (with a true value of $\eta_{\alpha\beta} = 0.1$) than DUNE. This discrepancy can be attributed to T2HK's substantial detector size (approximately 374 kton), which translates to enhanced statistical power.
- When considering a true value of $\eta_{\alpha\beta}$ equal to -0.1 , T2HK demonstrates superior constraints on the NSI parameters compared to DUNE, both at 3σ and 5σ confidence levels. This enhanced constraint in T2HK is anticipated because of its ability to gather a larger statistical sample owing to its large detector mass as compared to DUNE.
- In the joint analysis of DUNE+T2HK, the sensitivity for constraining the $\eta_{\alpha\beta}$ parameters improves significantly, leading to tighter bounds on $\eta_{\alpha\beta}$. The synergy between DUNE and T2HK consistently enhances the sensitivity due to the considerable combined data set from both detectors.

Figure 4.6 shows the constraining capabilities of DUNE, T2HKK, and the combined analysis DUNE+T2HKK for the $\eta_{\alpha\beta}$ parameters. The outcomes for η_{ee} , $\eta_{\mu\mu}$, and $\eta_{\tau\tau}$ are displayed in the left-panel, middle-panel, and right-panel, respectively. The plot represents $\Delta\chi^2$ as a function of the test $\eta_{\alpha\beta}$ parameter. Our observations are as follows:

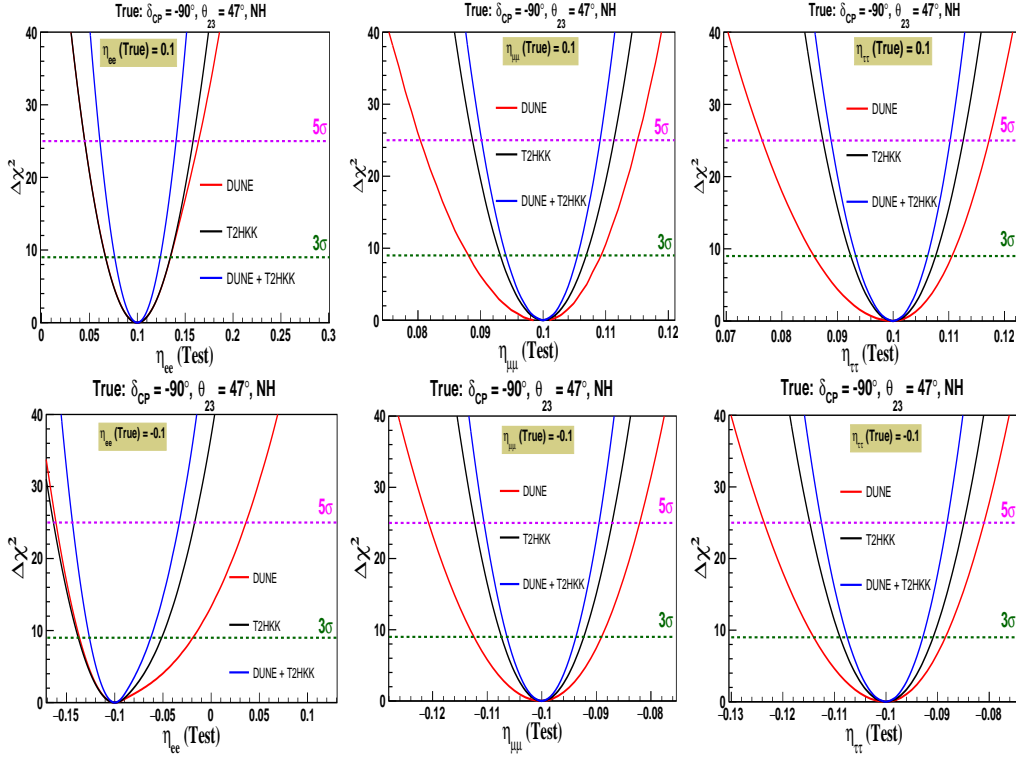


FIGURE 4.6: The sensitivity of DUNE, T2HKK and DUNE + T2HKK towards constraining η_{ee} (left-panel), $\eta_{\mu\mu}$ (middle-panel), and $\eta_{\tau\tau}$ (right-panel) at true $\delta_{CP} = -\pi/2$ and true $\theta_{23} = 47^\circ$. The top (bottom) panel is for true $\eta_{\alpha\beta} = 0.1$ (-0.1). In all the three plots the results for DUNE, T2HKK and DUNE+T2HKK are shown in red, black and blue respectively.

- The constraining potential of T2HKK is relatively weaker than that of DUNE for both η_{ee} and $\eta_{\mu\mu}$. In the case of $\eta_{\tau\tau}$, when the test value ($\eta_{\tau\tau}$) is less than or equal to the true value ($\eta_{\tau\tau}$), DUNE and T2HKK exhibit overlapping capabilities. For the remaining range of $\eta_{\tau\tau}$, DUNE surpasses T2HKK in terms of sensitivity.
- For the case with $\eta_{\alpha\beta} = -0.1$, we see that the sensitivity of T2HKK towards constraining the scalar NSI parameters is higher as compared to that of DUNE for both 3σ and 5σ confidence levels.
- The combination of DUNE and T2HKK results in a more robust constraint on $\eta_{\alpha\beta}$ compared to individual analyses of DUNE and T2HKK. This improved sensitivity is due to the substantial statistical power and the broader parameter space achieved through the synergy of DUNE and T2HKK.

4.6 Impact on CP Violation sensitivity

The pursuit of measuring the CP-violating phase δ_{CP} in the leptonic sector stands as a prominent objective for ongoing and upcoming neutrino experiments. The identification of CP violation (CPV) could hold vital implications for explaining the baryon asymmetry of the Universe, which pertains to the prevalence of matter over antimatter [169–171]. It is intriguing to delve into the secondary effects of scalar NSI on measurements associated with δ_{CP} within the neutrino sector. This discussion centers on the influence of $\eta_{\alpha\beta}$ on the CPV sensitivities at DUNE, T2HK, and T2HKK. The determination of sensitivities is accomplished by varying the genuine values of δ_{CP} within the permissible range of $[-\pi, \pi]$. The authentic values of other mixing parameters used in this analysis are enumerated in table 3.1. In the evaluation of sensitivity across δ_{CP} , only CP-conserving values, namely 0 and $\pm \pi$, are considered in the test spectrum. The process involves the marginalization of θ_{23} and Δm_{31}^2 over the allowed 3σ intervals, with subsequent minimization of the χ^2 value over all the ranges of marginalization. We define the CPV sensitivity the same as discussed in equation 3.2

In figure 4.7 we show the impact of scalar NSI on CP-violation sensitivity for DUNE (left column), T2HK (middle column), and the combined DUNE + T2HK scenario (right column). The inclusion of scalar NSI significantly impacts both DUNE and T2HK’s CPV sensitivity. The depicted graphs showcase the statistical significance σ ($=\sqrt{\Delta\chi_{CPV}^2}$) as a function of the true δ_{CP} . The top row displays the outcomes for η_{ee} , the middle row for $\eta_{\mu\mu}$, and the bottom row for $\eta_{\tau\tau}$. The χ^2 analysis encompasses marginalization over the NSI parameters. In all instances, the solid-red curve corresponds to the absence of scalar NSI ($\eta_{\alpha\beta} = 0$). The solid (dashed) black and blue curves denote the chosen positive (negative) values of $\eta_{\alpha\beta}$. The following observations are gleaned from figure 4.7:

- A positive (negative) η_{ee} predominantly heightens (attenuates) CPV sensitivities for both DUNE and T2HK. For $\eta_{ee} = 0.1$ and δ_{CP}^{true} within $[0, 90^\circ]$, the sensitivities with and without scalar NSI exhibit a substantial overlap. In the context of the DUNE + T2HK combined study, sensitivities (with and without NSI) are fortified across all cases, particularly in the overlapping region. This improvement can be attributed to the broader range of data collected from the combined detector ensemble.
- The presence of a positive $\eta_{\mu\mu}$ adversely affects CPV sensitivities in the upper half-plane of δ_{CP} , i.e., $[0, \pi]$, for DUNE. Conversely, the effect for the rest of the δ_{CP} range is characterized by mild fluctuations. At T2HK, a positive $\eta_{\mu\mu}$ is

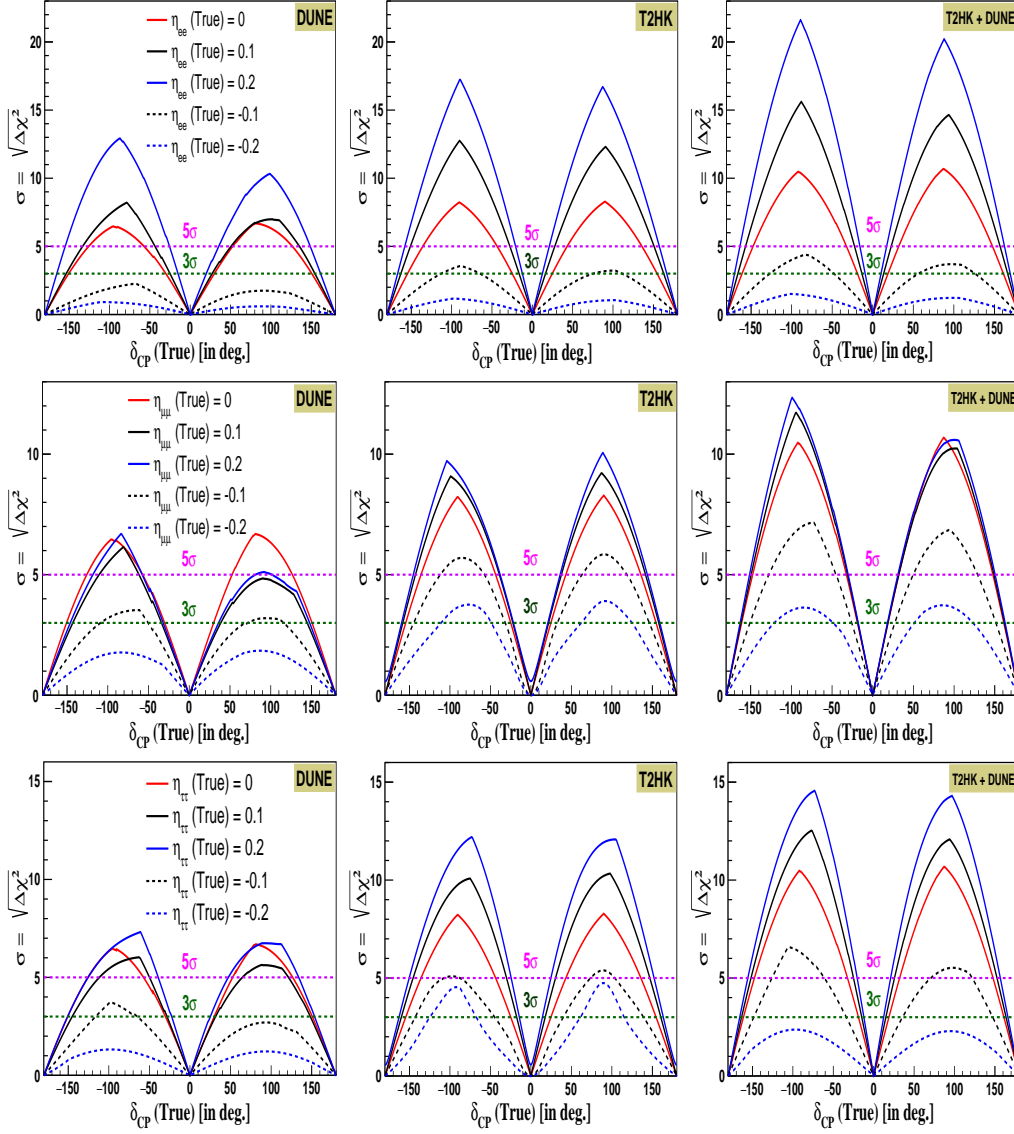


FIGURE 4.7: The CPV sensitivity of DUNE (left-column), T2HK (middle-column) and DUNE + T2HK (right-column) in presence of scalar NSI. The plots for η_{ee} , $\eta_{\mu\mu}$ and $\eta_{\tau\tau}$ are included in the top-row, middle-row and bottom-row respectively. The solid-red curve is for the no scalar NSI case whereas solid (dashed) black and blue curves are for positive (negative) $\eta_{\tau\tau}$.

associated with enhanced sensitivities. Negative $\eta_{\mu\mu}$ values, however, lead to a substantial dampening of sensitivities for both DUNE and T2HK. Remarkably, the combination of DUNE and T2HK augments overall sensitivities, regardless of the presence of NSI.

- Concerning DUNE, the introduction of a positive $\eta_{\tau\tau}$ yields marginal fluctuations when contrasted with the case without scalar NSI. T2HK, in the presence of positive $\eta_{\tau\tau}$, witnesses augmented sensitivity. The joint analysis of DUNE+T2HK results in heightened sensitivities, both with and without NSI.

In figure 4.8, we present the implications of scalar NSI on the CP-violation (CPV) sensitivities at DUNE (left-panel), T2HKK (middle-panel), and the joint analysis of DUNE + T2HKK (right-panel). Evidently, the influence of $\eta_{\alpha\beta}$ on CPV sensitivities is notably discernible for both DUNE and T2HKK. The collaborative approach enhances sensitivity due to the amalgamation of larger statistics from a broader spectrum of degenerate parameter spaces. The analysis encompasses the marginalization of NSI parameters and θ_{23} within the permitted interval $[40^\circ, 50^\circ]$. The solid red line signifies the standard scenario, while other solid (dashed) lines denote positive (negative) values of $\eta_{\alpha\beta}$. The impacts of η_{ee} , $\eta_{\mu\mu}$, and $\eta_{\tau\tau}$ are delineated in the top-panel, middle-panel, and bottom-panel respectively. The dashed green and dashed magenta lines denote the 3σ and 5σ confidence levels respectively. Our observations are as follows:

- A positive (negative) η_{ee} primarily enhances (diminishes) the CPV sensitivities for DUNE and T2HKK. In the interval $\delta_{CP}^{true} \in [0, 90^\circ]$, the sensitivities overlap between the cases of no scalar NSI and $\eta_{ee} = 0.1$. This implies that within this range, DUNE alone may not discernably differentiate genuine sensitivity from that arising due to scalar NSI. However, the joint analysis of DUNE + T2HKK holds the potential to eliminate this degeneracy and enhance the overall sensitivities (with and without NSI).
- A negative $\eta_{\mu\mu}$ hampers CPV sensitivity, whereas a positive $\eta_{\mu\mu}$ introduces various degeneracies in CP measurements. For instance, at T2HKK, standard CPV sensitivities overlap with NSI-induced sensitivities for $\eta_{\mu\mu} = 0.1$ within $\delta_{CP}^{true} \in [-180^\circ, -120^\circ]$ and $\delta_{CP}^{true} \in [110^\circ, 180^\circ]$. However, the joint analysis of DUNE + T2HKK can alleviate this degeneracy.
- A negative $\eta_{\tau\tau}$ suppresses CPV sensitivities, whereas a positive $\eta_{\tau\tau}$ predominantly enhances them. Notably, with a positive $\eta_{\tau\tau}$, the sensitivities with and without scalar NSI overlap across various regions of δ_{CP}^{true} . Consequently, the experiments' capacity to differentiate between standard and non-standard interactions becomes indistinguishable. The combined sensitivity of DUNE + T2HKK proves instrumental in alleviating this degeneracy, thereby enhancing overall CPV sensitivities (with and without NSI).

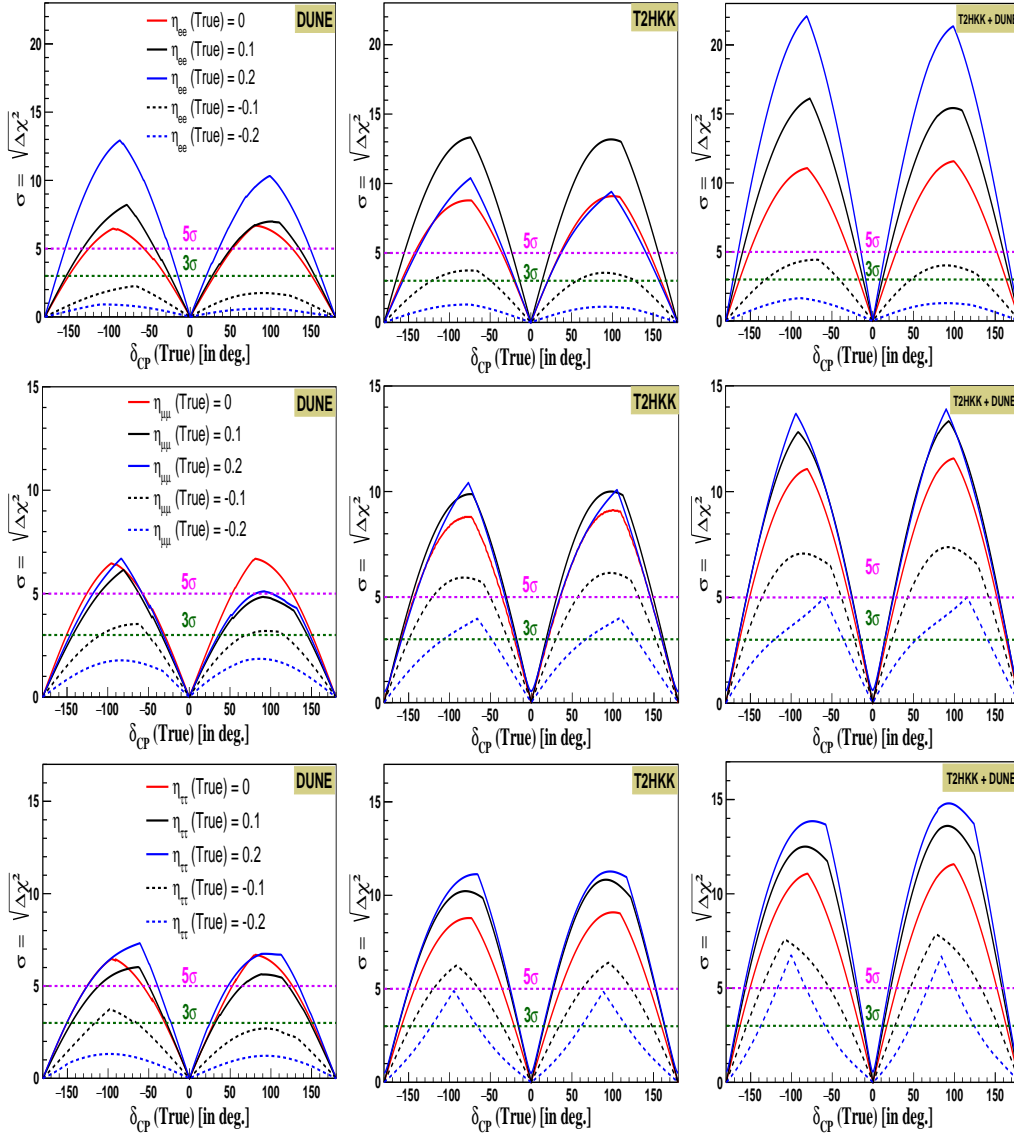


FIGURE 4.8: The CPV sensitivity of DUNE (left-column), T2HKK (middle-column) and DUNE + T2HKK (right-column) in presence of scalar NSI. The plots for η_{ee} , $\eta_{\mu\mu}$ and $\eta_{\tau\tau}$ are included in the top-row, middle-row and bottom-row respectively. The solid-red curve is for the no scalar NSI case whereas solid (dashed) black and blue curves are for positive (negative) $\eta_{\tau\tau}$.

4.7 Chapter Summary

With remarkable advancements in the realm of neutrino physics, coupled with cutting-edge experimental setups, there is a concerted effort to measure neutrino oscillation parameters with the utmost precision. The forthcoming flagship neutrino experiments have ambitious goals of achieving the most accurate determination of neutrino mixing parameters. Presently, among the least constrained parameters in neutrino physics are δ_{CP} and the octant of the mixing angle, θ_{23} .

This study primarily delves into the implications of scalar NSI on the sensitivity of CP measurements for three upcoming long-baseline (LBL) experiments: DUNE, T2HK, and T2HKK, in a model-independent manner. Moreover, we explore the advantages offered by combined analyses involving DUNE + T2HK and DUNE + T2HKK. In the presence of scalar NSI, a substantial impact on CP-violation sensitivity is observed. For chosen negative values of NSI parameters, a decrease in CP measurement sensitivity is evident. Interestingly, an overlap between standard and non-standard CPV sensitivities is noticed for specific positive $\eta_{\alpha\beta}$ values at DUNE and T2HKK. This implies that these experiments may not be able to distinguish between genuine CP effects and those arising from scalar NSI within those regions. However, the joint sensitivity analysis of DUNE + T2HK and/or DUNE + T2HKK is effective in resolving this issue, primarily due to the broader parameter space coverage. Furthermore, T2HK exhibits superior capabilities in constraining NSI parameters when compared to DUNE or T2HKK, mainly attributed to its sizable detector size (around 374 kton fiducial mass). The synergy between two experiments (DUNE + T2HK or DUNE + T2HKK) allows for the accumulation of substantial statistics over an expanded parameter space, consequently improving overall sensitivities for all non-zero NSI parameters. Notably, combining the outcomes of all three experiments showcases significant enhancements (or reductions) in CPV sensitivities for positive (or negative) $\eta_{\alpha\beta}$ values. Remarkably, the η_{ee} element emerges as the most sensitive with regard to CPV, across all considered NSI parameters.

Recognizing these subtle neutrino effects and their implications on the potential of various neutrino experiments is of utmost importance. This study primarily focuses on comprehending the influence of scalar NSI on three upcoming LBL experiments. We are also engaged in exploring the impact of NSI on other aspects of physics sensitivities in diverse neutrino experiments. A collaborative effort encompassing solar, atmospheric, reactor, and other experiments is essential to comprehensively understand the implications of NSI. Equally vital is the imposition of stringent constraints on the effects of scalar NSI to ensure accurate data interpretation across a range of neutrino experiments.

